Conceptual Design and Center-point Force Dynamic Simulation of a New Horizontal Axis Semi-exposed Wind Turbine

Nazim Mir-Nasiri *‡, Daniyar Seitenov **

* Department of Electrical and Electronics Engineering, School of Engineering, Nazarbayev University,

53, Kabanbay Batyr Ave., Astana, 010000, Kazakhstan

** Department of Electrical and Electronics Engineering, School of Engineering, Nazarbayev University,

53, Kabanbay Batyr Ave., Astana, 010000, Kazakhstan

(nazim.mir-nasiri@nu.edu.kz; dseitenov@nu.edu.kz)

‡ Corresponding Author; First Author, 53, Kabanbay Batyr Ave., Astana, 010000, Kazakhstan,

Tel: +77172709128, nazim.mir-nasiri@nu.edu.kz

Received: 03.11.2015 Accepted:01.10.2015

Abstract- Renewable energy sources are fast growing. Nowadays much effort has been made by inventors to devise new and more efficient configurations of wind turbines. This paper describes mechanical design and resultant-force dynamic simulation of innovative horizontal axis semi-exposed wind turbine structure. The innovation in wind turbine structure includes flat shape of its blades and their orientation towards the wind that minimizes the axial component of wind force on the shaft bearings. As a result, the wind power is fully utilized to generate a useful rotary force that drives the generator rotor. This enhances the efficiency of the turbine as compared to complex shape blades in traditional horizontal axis wind turbines. The distinctive feature of the system is also an oscillating shield that automatically protects the generator shaft from over speeding at extreme wind speeds, and therefore, from generating power above its nominal capacity. The over speeding may even cause a physical damage to the generator. The center-point force dynamic load models on the rotor blades have been derived for various wind conditions. The simulation algorithms have been tested in MATLAB Simulink environment. The results of simulation show the efficacy of the system and an advantage of using this system with the over speed shield protection.

Keywords Wind energy, horizontal axis turbine, dynamic simulation, over speed protection.

1. Introduction

The interest on renewable energy sources has been increased significantly during last decades. The reason is to decrease the air pollution, help on preventing global warming, save the natural resources and stable energy prices [1, 2]. Renewable energy sources are inexpensive and fast growing [3]. For the duration from 1996 to 2011 the production of electricity by using of wind turbines has been increased significantly. It was estimated by WWEA (World Wind Energy Association) that by the end of 2015 capacity of wind energy can go up to 600,000 MW. Currently a lot of effort is being made to find new and more efficient designs and configurations of wind turbines by different companies and universities all over the world [4, 5, 6]. In general, depending on position of the rotor with respect to the ground there are two types of wind turbines: horizontal axis wind turbine (HAWT) and vertical axis wind turbine (VAWT).

VAWT has different configuration and design types. The distinctive feature of VAWT is that there is no need to head it in to the direction of the wind, unlike HAWT [7]. The Darrieus type of VAWT was patented in 1931 by G.J.M. Darrieus and is the most efficient turbine among other VAWTs. This model has an easy construction and all the control mechanisms are located on the ground. The model does not require any yaw mechanism. The disadvantage of Darrieus WT is that it is not self starting wind turbine. Usually it is run by induction motor sourced from the grid. Darrieus WT was optimized and modified during the last 7 decades. Such as Giromill VAWT has a straight number of

blades from two up to five on it. Sometimes it is referred as a H-rotor [8, 9]. In Darrieus-Masgrove rotor VAWT the model is divided into two tiers. The straight blades of the top layer is placed 90° with respect to the bottom layer blades. Efficiency of this turbine is 39-40%. The blades on Darrieus-Masgrove turbine are wider, in order to achieve self starting in a lower speed of wind [10]. In Twisted three-bladed rotor VAWT Gupta and Biswas offered to increase the number of blades up to three and twist them in order to reduce the flow separation. The disadvantage of the model is complexity in producing twisted blades [11]. Apart from Darrieus VAWT there is Savonius VAWT. It is in half and hollow shaped cylinder form. This WT is easily self starts in comparison to other VAWT types. But because of the shape of the turbine the efficiency of turbine is lower than in Darrieus turbine and cannot be used as a commercial type of WT [10]. The Savonius turbines are used when the cost is at first and efficiency on second place. Combining the advantages of Savonius and Darrieus VAWTs has led to new type of efficient WT. The model combines the high value for starting torque of Savonius tubine and efficiency of Darrieus turbine. [12]. The Sistan VAWT was found in a modern part of Iran's territory. Sistan turbine can be easily integrated in a building [13]. The use the disc on the bottom and top of the rotor has enabled easy rotation and increased the efficiency of the turbine up to 30%.

The HAWT (usually with three blades) is mostly oriented to high speed wind and it covers 90% of all electricity generated by wind turbines. Generator and rotor's shaft usually connected with gearbox in order to obtain suitable speed rotation for generator. HAWTs are divided into two types: upwind and downwind. In upwind mode the wind firstly passes the blades and then passes the tower. The advantage is that there is a little possibility that the tower can effect on the coming wind. The disadvantage is that the rotor should be made of stark material in order to prevent the damage of a tower. For a big turbine of this kind it is preferable to use a yaw mechanism that will face the turbine in a direction of a wind, but for small ones it is possible to use the tail vane. The biggest aim for HAWT is to increase the output energy and decrease the cost for electricity [14, 15]. In a case of downwind wind turbines it is vice versa. The rotor stays after the tower, so the wind initially passes the tower and then passes the blades [16]. The advantages are that there is no need for a yaw mechanism and the rotor can be made of a flexible material that is not expensive to make. The other advantage is that there is less stress on a tower comparing to upwind wind turbines. In order to obtain the advantages from both types of turbines, many researchers focused on designing a combined type of wind turbines [17, 18].

The proposed design of a new horizontal axis semi-exposed wind turbine (HASWT) structure aims to increase the wind energy utilization as compared to modern HAWT and VAWT that have twisted shape of blades. Because of flat shape of its blades that are directly facing to a wind flow, this design minimizes the axial component of the wind force that adversely affects the rotor bearing and enables only a useful rotary component of driving force on the generator shaft. This will increase the efficiency of the turbine as compared to the traditional wind turbines where part of the wind force is actually affecting the rotor bearing.

2. Structural Design of Horizontal Axis Semi-exposed Wind Turbine (HASWT)

The 3D schematic view of the designed wind turbine system is shown in Fig 1. The turbine generator is located on an elevated rotary platform 1. The generator shaft 2 is mounted horizontally and fitted with four orthogonal and slightly convex at the edges (not shown in the figure) flat blades 3. There are two sets of such blades that are rigidly connected along the rotating shaft. The usage of two sets of blades instead of one helps to smooth the fluctuation of rotary speed of the shaft. Only two blades in each set are subjected to a stream of horizontal wind flow at any time. Thus the blades that are below the horizontal axis of the shaft are shielded from wind by the slopped shape platform 1. The platform 1, in turn, is connected to a vertical post 4 by means of thrust bearings and it is able to rotate about its vertical axis. The platform rotation is naturally controlled by the vertical tail fin 5 that is rigidly attached to it. The fin ensures that the blades are always facing to the direction of wind blow.

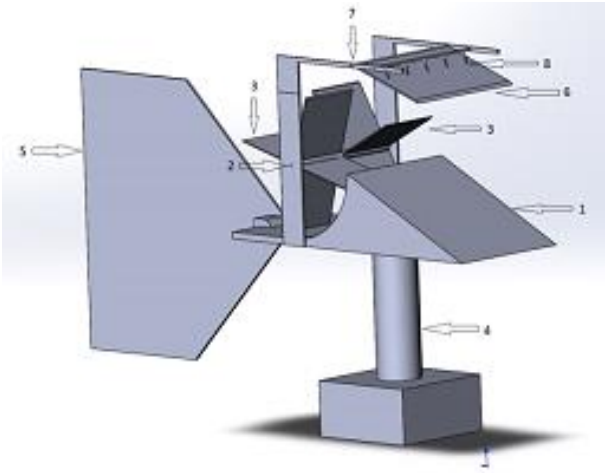

Fig. 1. Schematic view of the designed turbine system

The distinctive feature of the designed system is the oscillating shield 6. It is joined to the platform by means of horizontal hinge 7 and able to rotate about its axis. However, the amount of rotation is controlled by the set of tension springs 8 that connects shield 6 to platform 1. The details of the shield connections are shown in Fig. 2. In fact, the amount of shield rotation solely depends on strength of blowing wind and the selected spring constant. In non-deformed condition the springs are in the state of initial tension that prevents shield from being rotated. In this condition (acceptable wind speed) wind can easily pass the gap between shield 6 and platform 1, reach the generator blades and rotate the shaft with maximum power. If the wind speed increases beyond the set value, i.e. its value becomes sufficiently enough to overcome the initial tension, the spring will yield. The shied then turns and partially obstructs the wind passage to the blades. As a result, the gap becomes smaller and this, in turn, slows down rotor rotation at extreme (unacceptable) wind speeds. The more is the wind speed the less is the torque on the shaft. The convex shape of

the blade edge (not shown in Fig. 1) is additionally introduced to reduce the air turbulence at edges of the blades.

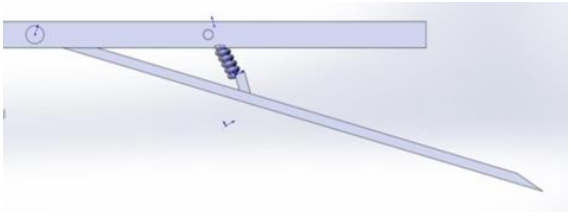

Fig. 2. Wind shield of the system

3. Center-point Force Analysis of HASWT

The general assumption made in this analysis is that the tail of the platform keeps the blades and shaft axis always perpendicular to the direction of wind blow. Therefore, the analysis of the dynamic forces and torques on the blades can be separated in two different cases:

- Normal wind speed conditions (no-shield involvement), when the shield springs are strong enough to keep the shield in its original position (i.e. it does not obstruct the wind at all)
- Extreme wind conditions (shield involvement) when the wind pressure is strong enough to turn the shield plate and as a result it will partially obstruct the wind stream

3.1 Modelling of Dynamic Forces under Normal Wind Speed Conditions

In this case shield springs are strong enough to resist the wind pressure. The wind has a full access to only two blades in each set, i.e. blades1 and 2. These blades appear above the center of rotation as shown schematically in Fig. 3. Blades 3 and 4 are hidden from wind by the platform structure. As a result, there will be a net torque applied on the rotor shaft. The wind also affects the shield 5. However, in this case the wind is not strong enough to stretch springs 8 (Fig.1) and, thus, change the position of the shield. In Fig 3 and other figures the wind streamlines are assumed to be strictly horizontal and does not show the real wind patterns and ensuing variable air pressure patterns that may appear at the boundaries of rigid obstacles. This may introduce some but minor errors in the simulation models. The purpose of this paper is to introduce a concept of new type of wind generator and prove its work principles and advantages.

Figure 4 shows (schematically) application of resultant wind forces F_1 and F_2 on two blades 1 and 2, respectively. Each resultant force F_i (where i=1, 2) depends on square value of wind speed. F_i is simply approximated as being applied normally at the geometric centers of each blade area C_1 and C_2 that are exposed to always horizontally oriented wind force F. The resultant force on a stationary vertically positioned blade is known from the classical fluid mechanics books [19] and other literature sources [20] and can be expressed as:

$$F_i = 1/2\ \rho\ C_d\ v^2\ A_i \qquad (1)$$

where:

ρ = 1.2 kg/m^3 is the air density at the sea level (selected for simulation);

C_d = 1.28 is the drag coefficient for a flat plates;

v is the wind speed with respect to the blades, m/sec;

A_i is the area of i-th blade that is subjected to the normal air pressure.

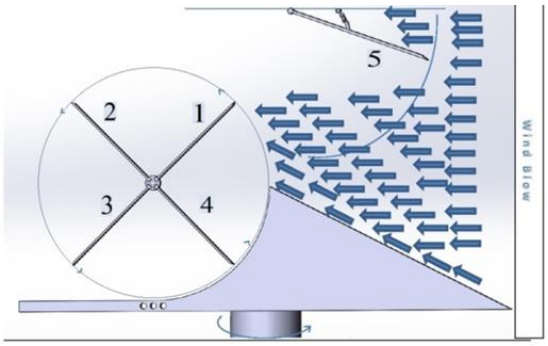

Fig.3. Blades under normal wind speed condition

In Fig. 4 each blade has width W_b and height H_b. The rotor blades are perpendicular to each other and the position of the rotor shaft could be defined uniquely by angle α that blade 1 makes with the reference axis X. We assume that the resultant of wind force F is parallel to horizontal axis X. Since the blades are not stationary but rather rotating the resultants of wind forces F_1 and F_2 (Fig. 4) are then rather results of wind speed values relative to the linear speed values of the rotating blades. As a reference point to define the linear speed of the blades we may take the point with the highest value of the linear speed, i.e. the blade tip point. Therefore, the relative wind speed v in (1) can be approximated as follows:

$$v = v_w - \omega \cdot H_b \qquad (2)$$

where

v_w is the absolute velocity of the wind;

ω is the angular velocity of the rotor blades.

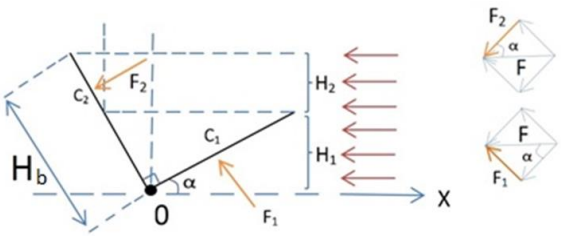

Fig.4. Wind forces applied on blades 1 and 2

From Fig. 4 it is obvious that only normal component of the horizontal force F drives the shaft. Therefore, the normal

components of resultant wind forces F_1 and F_2 at the centers of respective areas A_1 and A_2 depend on the actual angular position of the blades α and can be defined from (1) as follows:

$$F_1 = 1/2\ \rho\ C_d\ v^2\ A_1 \sin\alpha$$
$$F_2 = 1/2\ \rho\ C_d\ v^2\ A_2 \cos\alpha \quad (3)$$

If both blades have the same width W_b, then W_bH_1 and W_bH_2 become vertical projections of blade areas A_1 and A_2 that are subjected to the horizontal wind force F. From Fig. 4 it is obvious that the first blade area that is subjected to the wind is $A_1 = W_b \cdot H_b$ (no obstruction) and the second blade area that is subjected to the same wind is $A_2 = W_b \cdot H_b \cdot (\cos\alpha - \sin\alpha)/\sin\alpha$ (partially obstructed by the first blade). As long as area value A_2 has positive value, i.e. $\cos\alpha > \sin\alpha$, the second blade is exposed to wind. Otherwise, it will be fully obstructed by blade 1. Substituting A_1 and A_2 into equations (3) yields the following updated expressions for F_1 and F_2:

$$F_1 = (1/2)\ \rho\ C_d\ v^2\ W_b \cdot H_b \sin\alpha$$
$$F_2 = (1/2)\ \rho\ C_d\ v^2\ W_b \cdot H_b \cdot (\cos\alpha - \sin\alpha) \quad (4)$$

The rotary torques generated by center-point forces F_1 and F_2 depend on the positions of area centers C_1 and C_2 on the blades. The positon of C_1 on the first blade does not change with time whereas the position of C_2 on the second blade varies because the area A_2 reduces with time as shown in Fig. 4. The moment arms of forces F_1 and F_2 are OC_1 and OC_2, respectively. Using the geometry T_1 and T_2 can be derived from Fig. 4 as follows:

$$T_1 = F_1 \cdot H_b/2 = (1/4)\ \rho\ C_d\ v^2\ W_b \cdot H_b^2 \sin\alpha \quad (5)$$

$$T_2 = F_2 \cdot [H_b - (1/2) \cdot H_b \cdot (\cos\alpha - \sin\alpha)] =$$
$$= (1/4)\ \rho\ C_d\ v^2\ W_b \cdot H_b^2 [(\cos\alpha)^2 - (\sin\alpha)^2] / \cos\alpha \quad (6)$$

Finally, the net positive torque on the generator shaft under normal wind speed conditions can be calculated as by adding T_1 and T_2.

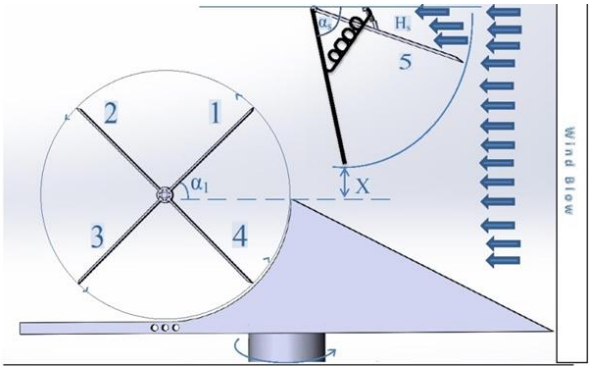

Fig.5. Blades under extreme wind speed condition

3.2 *Modelling of Dynamic Forces under Extreme Wind Speed Conditions*

In this case the wind speed is strong enough to overcome the initial tension of the spring and forces it to extend. As a result, the shield will turn and reduce the volume of air reaching the blades as shown in Fig 5. In Fig 5 H_b is length of the blades, H_S is length of the shield, x is amount of opening (gap) for the wind to reach the blades, and α_S is angular position of the shield with respect to the horizontal axis. The more is α_S the less is gap size x. Consequently, the less is x the less is air volume reaching blades 1 and 2. The wind force applied on blade 1 depends on both, angular position of blade 1 (α_1) and angular position of the shield (α_S) as shown in Fig. 6.

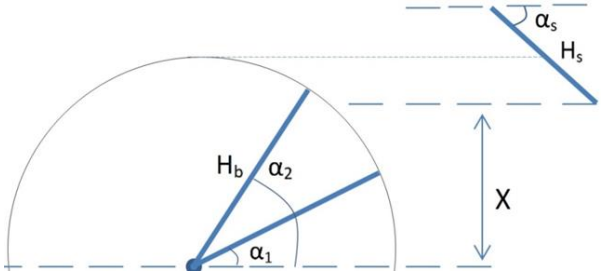

Fig.6. Blade 1 in two different positions, angles α_1 and α_2

There are two distinct cases of blade 1 angular locations. In the first case the blade angle is α_1 and in the second one when the blade is at angle α_2 (Fig. 6). For angle α_1 the entire area of the blade is exposed to the wind force. Therefore, the following inequalities are true:

$$H_b \cdot \sin\alpha_1 \le x \text{ or } H_b \cdot \sin\alpha_1 \le H_S (1 - \sin\alpha_S) \quad (7)$$

In this case there is no shield obstruction for the wind to reach blade 1. Therefore the driving torque T_1 on blade 1 can be calculated from equation (5). However, for the second position angle α_2 only part of the blade area is exposed to the wind force (Fig. 6). Therefore for this case the opposite to (7) inequalities are held true

$$H_b \cdot \sin\alpha_2 > x \quad \text{or} \quad H_b \cdot \sin\alpha_2 > H_S (1 - \sin\alpha_S) \quad (8)$$

In this case the wind access to the blade 1 is restricted to the amount of opening x only. Therefore, the area of the first blade that is really subjected to the wind can be calculated as

$$A_1 = \frac{H_S \cdot (1 - \sin\alpha_S)}{\sin\alpha_2} \cdot W_b \quad (9)$$

The normal wind force at the center of area A_1 can be calculated as

$$F_1 = 1/2\ \rho\ C_d\ v^2\ A_1 \cdot \sin\alpha_2 \quad \text{or}$$
$$F_1 = 1/2\ \rho\ C_d\ v^2 \cdot H_S (1 - \sin\alpha_S) \cdot W_b$$

Finally, the driving torque on blade 1 due to the force F_1 (as assumed to be applied at the center of the area A_1) can be calculated as

$$T_1 = F_1 \cdot 1/2 \cdot \frac{H_S \cdot (1 - \sin\alpha_S)}{\sin\alpha_2} =$$
$$= 1/4\ \rho\ C_d\ v^2\ W_b \cdot \frac{H_S^2 \cdot (1 - \sin\alpha_S)^2}{\sin\alpha_2} \quad (10)$$

The driving torque applied on blade 2 depends on angular position of both blades and the angular position of the shield α_s as shown in Fig. 7.

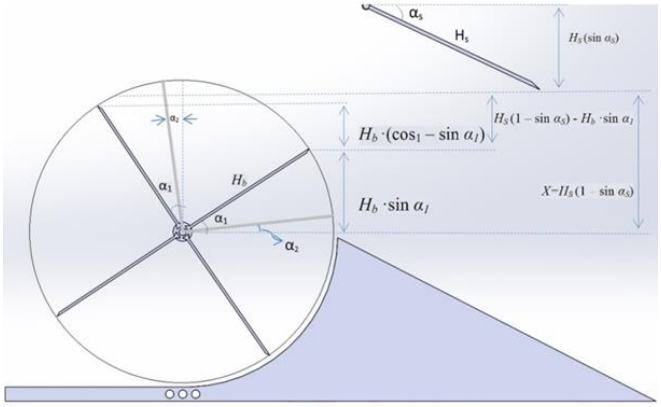

Fig.7. Blade 2 in two different positions, angles α_1 and α_2

There can be identified two distinct cases of blade 2 angular locations for the force analysis. One of them is angle α_1 and the second one is angle α_2 (Fig. 7). For a given angle α_1 the following inequalities are held true:

$$H_b\cdot(\cos_1 - \sin\alpha_1) \le H_S(1-\sin\alpha_S) - H_b\cdot\sin\alpha_1 \text{ or}$$
$$H_b\cdot\cos\alpha_1 \le H_S(1-\sin\alpha_S) = x \quad (11)$$

In this case there is no obstruction for the wind to reach both blade 1 and 2. Therefore the torque on the second blade T_2 can be calculated from equation (6). However, for the angular position α_2 (Fig. 7) the condition has changed as follows:

$$H_b\cdot\cos\alpha_2 > H_S(1-\sin\alpha_S) = x \quad (12)$$

The wind can access the entire area of blade 1 but partially the area of blade 2. Then area A_2 of blade 2 that is subjected the wind can be calculated as follows:

$$A_2 = \frac{H_S\cdot(1-\sin\alpha_S) - H_b\cdot\sin\alpha_2}{\cos\alpha_2}\cdot W_b \quad (13)$$

The normal wind force on the second blade the can be calculated as:

$$F_2 = 1/2\ \rho\ C_d\ v^2\cdot A_2\cdot\cos\alpha_2 \text{ or}$$
$$F_2 = 1/2\ \rho\ C_d\ v^2\cdot W_b\ [H_S(1-\sin\alpha_S) - H_b\cdot\sin\alpha_2] \quad (14)$$

Finally the driving torque on blade 2 due to the wind force F_2 (which is assumed to be applied at center of the affected area A_2) can be calculated as follows:

$$T_2 = F_2\left\{\frac{H_b\sin\alpha_2}{\cos\alpha_2} + \frac{1}{2}\cdot\frac{H_S(1-\sin\alpha_S) - H_b\sin\alpha_2}{\cos\alpha_2}\right\}$$

After reducing it can be written as:

$$T_2 = 1/2\ \rho\ C_d\ v^2\cdot W_b\cdot\left\{\frac{[H_S(1-\sin\alpha_S)]^2 - [H_b\sin\alpha_2]^2}{2\cos\alpha_2}\right\} \quad (15)$$

Finally, the net positive torque on the generator shaft under extreme wind speed conditions can be calculated by adding T_1 and T_2.

3.3 Roller bearing friction resistance on the rotor shaft

The roller bearing is assumed in the design because the force it takes to bring the object to the verge of moving from static condition can be hundred times less than that of a sliding bearing. The constant resistance to rotation of the shaft torque due to bearing friction can be expressed as follows:

$$T_b = \frac{1}{2}\cdot\mu\cdot P\cdot d \quad (16)$$

where:

μ is the coefficient of bearing friction ($1.2\ 10^{-3}$ for the roller bearing)

P is the bearing load that depends on the weight of the rotor, N

d is the bearing base size, m.

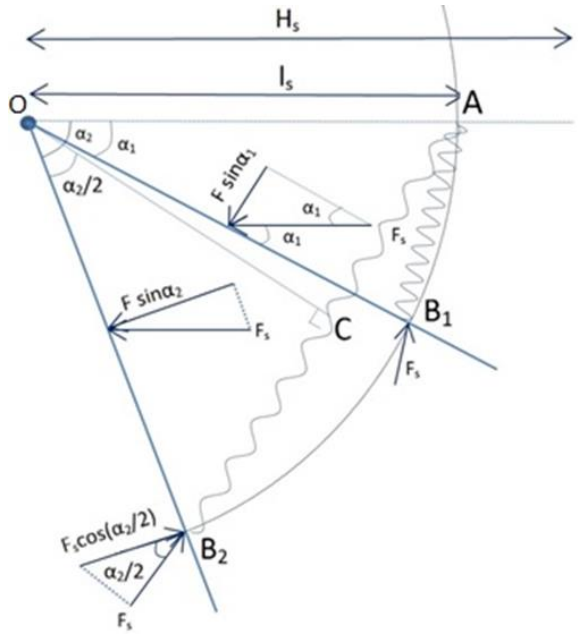

Fig.8. Initial and final positions of wind shield

3.4 Modelling of the Wind Shield Dynamics

Figure 8 shows initial (non-deformed spring with angle α_1) and final (deformed spring with angle α_2) positions of the wind shield. The amount of opening x (Fig. 6) depends on the net wind force applied on the shield surface and the selected retention spring stiffness k. The actual linear spring deformation d (Fig. 8) can be calculated as follows:

$$d = AB_2 - AB_1$$

where AB_1 is non-deformed spring length and AB_2 is deformed spring length. From Fig. 8 it is obvious that:

$$AB_1 = 2\, l_S \cdot \sin(\alpha_1/2) \text{ and} \quad (17)$$

$$AB_2 = 2\, l_S \cdot \sin(\alpha_2/2) = AC + CB_2 \quad (18)$$

where $l_S = OA$ is the distance from pin O to the point A where spring is attached to the shield. Therefore,

$$d = AB_2 - AB_1 = 2\, l_S \cdot [\sin(\alpha_2/2) - \sin(\alpha_1/2)] \quad (19)$$

The shield final angle α_2 due to strong wind force can be defined from torque balance equation on the shield with respect to pin point O.

$$H_s/2 \cdot F \cdot \sin(\alpha_2) = l_S \cdot F_S \cdot \cos(\alpha_2/2) \quad (20)$$

where F is the wind force at middle point C of the shield and F_S is axial load on the extended spring. Rewriting (20) yields:

$$H_s/2 \cdot F \cdot 2 \cdot \sin(\alpha_2/2) \cdot \cos(\alpha_2/2) = l_S \cdot F_S \cdot \cos(\alpha_2/2) \text{ or}$$
$$H_s/2 \cdot F \cdot 2 \cdot \sin(\alpha_2/2) = l_S \cdot F_S \quad (21)$$

Since the spring can be selected based on the maximum suggested load F_S^{max}, initial length of the spring AB_1 and the suggested maximum deflection or deformation of spring d^{max} the equations (17) and (18) can be used to define l_S and α_2. If, AB_1 is the initial length of non-deformed spring then $AB_2 = AB_1 + d^{max}$ is the maximum allowed length of deformed spring. Then dividing (18) by (17) yields the following expression:

$$\frac{AB_2}{AB_1} = \frac{\sin(\frac{\alpha_2}{2})}{\sin(\frac{\alpha_1}{2})} \quad (22)$$

From (22) we can derive expression for maximum allowed angular rotation of the shield $\propto_2^{max}$:

$$\propto_2^{max} = 2 \cdot \sin^{-1}\left[\frac{AB_1 + d^{max}}{AB_1} \cdot \sin\left(\frac{\alpha_1}{2}\right)\right] \quad (23)$$

The distance l_S then can be defined from (17) as follows:

$$l_S = \frac{AB_1}{2 \cdot \sin(\frac{\alpha_1}{2})} \quad (24)$$

Expression (21) can be used to define also the number n of springs connected in parallel that can share the total load applied to the shield by wind. Then F_S should be replaced by $F_S = F_S^{max} \cdot n$, where F_S^{max} is the maximum load allowed for a single spring. As well, F should be replaced in (21) by its maximum allowed wind force $F_{max} = 1/2 \cdot \rho \cdot C_d \cdot v_{max}^2 \cdot (W \cdot H_S)$, where v_{max} is the maximum selected wind speed, W is the width of the shield (it is same as the combined width of two sets of blades), and H_S is the height of the shield. Then the maximum number of springs in parallel n^{max} that is needed to balance forces F_{max} and F_S^{max} can be defined from (21) as follows

$$H_s/2 \cdot F_{max} \cdot 2 \cdot \sin(\alpha_2/2) = l_S \cdot (F_S^{max} \cdot n_{max}) \text{ or}$$

$$n_{max} = \frac{H_S \cdot F_{max} \cdot \sin(\frac{\alpha_2}{2})}{l_S \cdot F_S^{max}} \quad (25)$$

The springs should be equally spaced along the width W of the shield. v_{max} is the maximum speed that will cause deflection of the shied by angle α_2 (Fig 8). For the speed values less than v_{max}, i.e. for the forces F_i less than the maximum force F_{max}, equation (21) can be written as:

$$H_s \cdot (F_i - F_{min}) \cdot \sin(\alpha_2/2) = l_S \cdot (F_S \cdot n) \quad (26)$$

where F_{min} is the minimum wind force that will initiate the deformation of spring and deflection of shield. It depends on the initial tension force $F_{i,t}^S$ that the spring is able to hold without being deformed. $F_{i,t}^S$ is provided in the spring manufacturer's specification. According to Hook's law $F_S = d \cdot k$, where k if spring deflection rate from the specification and d is spring deformation value. By substituting F_S into (26), the spring deformation can be defined as a function of shield deflection angle α_2.

$$d = \frac{H_s \cdot (F_i - F_{min}) \cdot \sin(\frac{\alpha_2}{2})}{l_S \cdot n \cdot k} \quad (27)$$

By equating (27) and (19) the expression for the deflection angle α_2 can be derived as:

$$\sin\frac{\alpha_2}{2} = \frac{\sin(\frac{\alpha_1}{2})}{1 - \frac{H_S \cdot (F_i - F_{\min})}{2 \cdot l_S^2 \cdot k \cdot n}} \quad (28)$$

Formula (28) can be used to define the current angular position of the shield based on the selected values of α_1, H_s, k and calculated values of F_i, F_{min}, l_S and n. F_{min} can be defined independently from the following torque balance equation for the initial angle:

$$H_s \cdot F_{min} \cdot \sin(\alpha_1/2) = l_S \cdot (F_{i,t}^S \cdot n) \quad (29)$$

There is no deflection of the spring as long as $F_i < F_{min}$ and formula (28) should be used in case of $F_i > F_{min}$. From (29) F_{min} can be defined as follows:

$$F_{min} = \frac{l_S \cdot n \cdot F_{i,t}^S}{H_S \cdot \sin(\frac{\alpha_1}{2})} \quad (30)$$

On the other hand F_{min} corresponds to the minimum wind speed value that would be able to initiate the spring deflection, i.e.:

$$F_{min} = 1/2 \cdot \rho \cdot C_d \cdot v_{min}^{\,2} \cdot (W \cdot H_S) \quad (31)$$

By equating (30) and (31) the minimum wind speed value v_{min} can be defined as follows:

$$v_{min} = \sqrt{\frac{l_S \cdot n \cdot F_{i,t}^{S}}{\frac{1}{2} \cdot \rho \cdot C_d \cdot (W \cdot H_S^2) \cdot \sin(\frac{\alpha_1}{2})}} \quad (32)$$

The number of springs can be less than the maximum required to balance the maximum possible wind force, i.e. $n < n_{max}$. Then the maximum allowed shield angular deflection α_2 will be reached before the wind force reaches its maximum value, i.e. $F_i < F_{max}$. Therefore, there must be a stopper on the shield installation that will not allow the spring to deflect beyond its allowed deflection value, i.e. $d < d_{max}$. The wind speed value that corresponds to the maximum allowed deflection of n_i springs in parallel can be defined as follows:

$$v_{max} = \sqrt{\frac{l_S \cdot n_i \cdot F_S^{max}}{\frac{1}{2} \cdot \rho \cdot C_d \cdot (W \cdot H_S^2) \cdot \sin(\frac{\alpha_2}{2})}} \quad (33)$$

where α_2 is from (23) and F_S^{max} is the maximum load allowed on a single spring.

4 Computer Simulation of HASWT Operation

The simulation is based on the second Newton's law of rotational object as follows

$$\sum T = J \cdot \frac{d^2\alpha}{dt^2} \quad (34)$$

where $\sum T$ is the net torque on the shaft of the turbine, J is the moment of inertia of the shaft. For simplicity we may assume the rotor is a solid cylinder with mass m and radius r. Therefore, the moment of inertia of the cylinder can be expressed as $J=1/2 \cdot m \cdot r^2$. $\sum T$ depends on actual angular position α of the rotor blade 1 and angular position α_S of the shield (Fig. 3). $\sum T$ can be formed either by T_1 and T_2. These torques are calculated either from (5) and (6) if there is no obstruction by the shield or from (10) and (15) if there is an obstruction instead. The resistance to the rotor rotation is also formed by bearing friction torque T_b as it is calculated from (16). The shaft damping effect has not been taken into the account for this simulation and resistance torque T_G of the running generator is presented in accordance with its specified power rating. Therefore $\sum T$ can be expressed as

$$\sum T = T_1 + T_2 - T_b - T_G \quad (35)$$

The basis for simulation of shaft's angular position α and angular speed ω is the second Newton's law for rotational object (34) which is subjected to net torque (35). The program checks the conditions (7), (11) and calculates right values for T_1 and T_2 either from formulas (5) and (6) or (10) and (15). The effective relative wind speed v is taken from formula (2). While the rotational speed of the shaft and blades increases the applied forces on blades 1 and 2decrease due to the reduction of relative speed v. As a result, with time the shaft rotational speed ω stabilizes and remains constant for a given constant speed v_w of the wind (2). The additional condition for the simulation is that the calculated angle α is used only within the range from 0 to 90 degrees. The loading of the shaft blades by the wind (35) is repeated only every first quarter of circular shaft rotation because there are only four orthogonal blades in each set and each blade is exposed to wind only during the first quarter of shaft rotation. The remainder function in MATLAB effectively splits continuously growing angle α into the sequence of rising angles from 0 to 90 degrees. As a result, sin α and cos α functions in the all formulas are calculated only for the first quarter of the shaft rotation in repetitive manner.

The simulation is conducted based on the rotor of Kingspan Wind KW6 wind turbine. According to the specification it has a pick power generation of 6.1 kW, rotor shaft radius of 1.2 m and mass around 6000 kg. The selected two sets of blades have 2 m width and 4 m height (Fig. 1). The shield width is selected to be W_S = 4 m wide to cover both blade sets. The maximum wind speed that causes full stretch of the shield is selected to be v_{max} = 25 m/sec. The selected shield spring TSS: PE208 characteristics are shown in Table 1. Blade height H_b = 4m defines the height of shield H_S =6.07 m. That means shield should be able to fully cover both blades if turned to 90° from its arbitrary selected initial angle α_1=20°. However, the selected type of the springs (Table 1) will not be able to provide rotation of shield up to 90° at the maximum wind speed v_{max} = 25 m/sec due to the limitation of maximum spring deflection and maximum allowed spring load. The maximum angular rotation of the shield from its initial angle α_1=20° then can be calculated from (23), i.e. α_2^{max} = 35.4° which will close almost half of the wind access to the blades when the wind speed reaches v_{max} = 25 m/sec.

Table 1. Selected spring parameters

Length, (AB_1), mm	Rate, (k), N/mm	Max. deflection, (d^{max}), mm	Max. Load, (F_S^{max}), N	Initial tension, (F_{min}), N
190.5	4.4	143	683	57

The distance l_S from pin O to the point of spring attachment A on the shield can be defined from (24), l_S = 0.55 m. The maximum number of parallel springs n^{max} that is needed to balance maximum wind force F_{max} (at maximum wind speed) and F_S^{max} can be defined form (25), i.e. n^{max} = 57. Values of α_2 vary and depend on actual wind speed and are calculated from (28). Formula (32) defines the minimum wind speed value v_{min} that initiates the deflection of all parallel springs, i.e. v_{min} = 9.5 m/sec. Formula (33) defines wind speed value that corresponds to the maximum allowed

deflection of n_i springs in parallel, i.e. v_{max}= 25 m/sec. All the obtained parameters are summarized in the Table 2.

Table 2. Blades, shield and spring parameters

Blades width and height (W_b x H_b), m	Shield width and height (W_S x H_S), m	Shield initial and max. angles (α_1 and α_2^{max}), deg	Maxim. number of springs (n^{max})	Springs attachment distance (l_S), m
2 x 4	4 x 6.07	20 and 35.4	57	0.55

Figure 9 shows the results of system dynamics simulation on the basis of formula (34) for a range of wind speeds from 2 m/sec to 26 m/sec. This graph shows the effect of wind speed on the rotation of blades with the shield in place (solid line) and without the shield (dash line). Both lines are obtained according to the same values of electromagnetic resistance loads/torque (due to the electric power generation) at the corresponding wind speed values. The graph clearly shows the advantage of shield as an automatic break for extreme wind speed values of 15 m/sec and above.

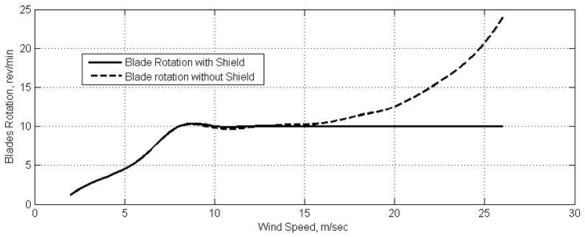

Fig.9. Blades rotation versus wind speed graph

Figure 10 shows the mechanical power generated by the system for a range of wind speed from 2 m/sec to 26 m/sec and corresponding rotational speed of the blades (Fig. 9). Solid line in the graph shows the electromagnetic torque applied to the shaft while the wind speed is kept increasing. Dash line demonstrates the power generated by the system when shield is in place. Dotted line shows the power generated by the same system when shield is not used. It is obvious that with the same load applied on the shaft the maximum power generated by the system with the shield does not exceed approximately the rated value of generator (6.1 kW), whereas when the system runs without shield, it attempts to produce a power that is much larger than the rated value (15 kW). So it may not utilize effectively the wind energy and unnecessarily increase rotor speed (Fig. 10) at extreme wind speeds.

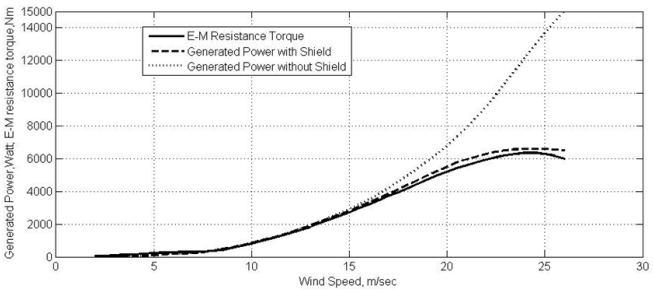

Fig.10. Power generation at various wind speeds

5. Conclusion

The developed HASWT system is able to fully utilize the wind energy because the wind forces applied on the blades generate only radial rotating torque on the shaft and no components of the force are generated in axial direction of the shaft. The vertically oriented tail of the platform, like a rudder of the airplane, enables the system to keep its rotor axis strictly perpendicular to the wind direction due to the balance of forces on both sides of the tail. This enables increasing the efficiency of wind power absorption. The important part of the design is the wind shield that is able to automatically protect the generator shaft at extreme wind speeds from over speeding and generating the power that is above the generator capabilities. The simplified point-force dynamic load models on the blades of the rotor have been derived for various wind conditions to demonstrate the potentials of this new HASWT wind turbine structure. The developed algorithms have implemented in MATLAB Simulink. The obtained results (Figs 9 and 10) show the efficacy of the system and the advantage of using the system with the preselected shield protection. The designed system has compact design and does not require any power consumption. It can be easily installed on the flat roofs of high-rise buildings for harvesting of wind energy. It is suitable for low and medium power generation because for high power generation it requires significantly longer and wider blades dimensions which could be a problem for their installation on the roof of high-rise buildings.

References

[1] A. C. Marques, and , J. A. Fuinhas, "Is renewable energy effective in promoting growth?", Journal of Energy Policy, 46(C), 2012, pp. 434-442 (Article)

[2] M. R. Moore, McD. L. Geoffrey, J. C. Daniel, "Markets for renewable energy and pollution emissions: Environmental claims, emission-reduction accounting, and product decoupling", Journal of Energy Policy, 2010, pp. 5956-5966 (Article)

[3] JR. Baker, "Features to aid or enable self-starting of fixed pitch low solidity vertical axis wind turbines", Journal of Wind Engineering and Industrial Aerodynamics, 15, 2003. Pp.369–80 (Article)

[4] S. Mathew, G.S. Philip, Wind turbines: evolution, basic principles, and classifications, Comprehensive Renewable Energy. Oxford: Publisher Elsevier, 2012, pp. 93–111 (Book)

[5] T.K. Barlas, G.A.M. van Kuik, "Review of state of the art in smart rotor control research for wind turbines", Progress in Aerospace Sciences, 46(1), 2010, pp. 1–27 (Article)

[6] M. Balat, "A review of modern wind turbine technology", Energy Sources, Part A: Recovery, Utilization, and Environmental Effects, 31(17), 2009, pp. 1561–1572 (Article)

[7] T. Chaichana, S. Chaitep, "Wind power potential and characteristic analysis of Chiang Mai, Thailand", Mechanical Science and Technology 24, 2010, pp. 1475–1479 (Article)

[8] R. Howell, N. Qin, J. Edwards, N. Durrani, "Wind tunnel and numerical study of a small vertical axis wind turbine", Renewable Energy 35, 2010, pp. 412–422 (Article)

[9] S. Mertens, G. van Kuik, G. van Bussel, "Performance of an H-Darrieus in the skewed flow on a roof", Journal of Solar Energy Engineering, 125, 2003, pp. 433–441(Article)

[10] D.N. Gorelov, V.P. Krivospitsky, "Prospects for development of wind turbines with orthogonal rotor", Thermophysics and Aeromechanics, 15, 2008, pp. 153–157(Article)

[11] R. Gupta, A. Biswas, "Computational fluid dynamics analysis of a twisted three bladed H-Darrieus rotor", Renewable and Sustainable Energy, 2010, pp. 1–15(Article)

[12] B.K. Debnath, A. Biswas, R. Gupta "Computational fluid dynamics analysis of a combined three-bucket Savonius and three-bladed Darrieus rotor at various overlap", Journal of Renewable and Sustainable Energy, 1, 2009, pp. 1–13(Article)

[13] G. Muller, F. Mark, M.F. Jentsch, E. Stoddart, "Vertical axis resistance type wind turbines for use in buildings", Renewable Energy, 34, 2009, pp. 1407–1412(Article)

[14] L. Wenzhi, Z.H Fuhai, W. Jianxin, L. Changzeng, "3D modeling methods of aerodynamic shape for large-scale wind turbine blades", IEEE International conference on information technology and computer science, Kiev, pp. 7–10, 25-26 July 2009. (Conference paper)

[15] C.A. Morgan, A.D. Garrad, "The design of optimum rotors for horizontal axis wind turbines, wind energy conversion", Tenth BWEA wind energy conference: Mechanical Engineering Publications Ltd., London, 1988, pp. 143–147 (Conference paper)

[16] T. Wang, F. Coton, "A high resolution tower shadow model for downwind wind turbines", Journal of Wind Engineering and Aerodynamics, 89(10), 2001, pp. 873–892

[17] E. Hau, Wind Turbines: Fundamentals, Technologies, Application, Economics, 2nd Ed., Springer-Verlag, Berlin, ,2006 (Book)

[18] S. N. Jung, T. S. No, K. W. Ryu, "Aerodynamic Performance Prediction of a 30kW Counter-rotating Wind Turbine System", Renewable Energy, 30, 2005, pp. 631–44(Article)

[19] Y. A Cengel, J. M. Cimbala, Fluid Mechanics: Fundamentals and Applications, 3rd edition, McGraw-Hill, 2103 (Book)

[20] H. N., Hristov, "Wind Turbines Introduction", Technical University Gabrovo, http://www.fh-schmalkalden.de/schmalkaldenmedia/wind+turbines.pdf E. (Article)